Modeling the SAR Signature of Nonlinear Internal Waves

FINAL REPORT

Grant Number: N00014-05-1-0368

Ellen E. Lettvin
Applied Physics Laboratory
University of Washington

OBJECTIVES AND IMPORTANCE

Nonlinear Internal Waves are pervasive globally, particularly in coastal waters. The currents and displacements associated with internal waves influence acoustic propagation and underwater navigation, as well as ocean transport and mixing. Synthetic Aperture Radar (SAR) imagery can reveal the surface manifestations of internal waves (IWs) in satellite imagery and so is routinely used to locate and characterize these features. Though some of the mechanisms that link the SAR signatures, surface processes, and the underlying internal structures have been understood for decades, a complete characterization has yet to emerge, making SAR imagery useful only as a qualitative tool. The objective of this research is to develop and validate a forward model to predict the SAR signature of NLIWs that explicitly includes relevant mechanisms that impact the sea surface roughness and corresponding backscattering cross section, such as wind speed and direction, compound modulation (i.e. modulation of intermediate-scale waves by IWs, which in turn modulate smaller waves), microscale breaking and breaking waves.

SIGNIFICANT RESULTS AND LESSONS LEARNED

1. Background

For the first part of this effort we developed a computationally efficient, web-based implementation of the Lyzenga and Bennett (1988) (LB) model, which uses the action balance equation to model the interactions between surface waves and currents, such as those generated by the passage of an IW. The action balance equation can be expressed, in general as:

$$\frac{\partial N(k)}{\partial t} + (c_{gi} + u_i)\frac{\partial N(k)}{\partial x_i} - k_j \frac{\partial u_j}{\partial x_i}\frac{\partial N(k)}{\partial k_i} = Q(k)/\omega \qquad (1)$$

where N(k) is the wave action spectrum (see Phillips, 1980) at a given wavenumber, k; Q(k) is the action source term that includes contributions from wind input, wave interactions and dissipative processes; x indexes spatial location along the current profile attributable to an IW, ω is the radian frequency, c_{gi} is the group velocity and u_i is the current due to the internal wave in the direction indexed by x.

In LB, the action balance equation is governed by a source function that considers energy input from the wind and viscous dissipation, of the form:

$$-\beta\frac{A}{Ao}(A-Ao), \tag{2}$$

where $\beta = 0.04\left(\frac{u*}{c}\right)^2 \omega|\cos(\phi-\phi_w|$ is the wave growth relaxation rate from Plant (1982), u* is friction velocity, c is phase velocity (c=ω/k), ω is radian frequency and ϕ_w is the wind direction. The term Ao is the equilibrium, or unperturbed spectrum for wind-generated surface waves. A refers to the perturbed surface waves that have been modulated by an internal wave. The ratio of A/Ao can be used to characterize the modulation of surface waves by currents from IWs. Examples of A/Ao for waves of various scales, ranging from centimeter-scale to tens of meters, for a given current profile are shown in Figures 1 and 2.

For the LB model, the equilibrium spectrum Ao is given by:

$$N(kx,ky) = B\exp\left(-2\left[\frac{ko}{k(kx,ky)\cos(\phi(kx,ky)-\phi_w)}\right]^2\right) \tag{3}$$

$$D(kx,ky) = \omega(k)\left\{k(kx,ky)^2 - 2k_1k(kx,ky)\cos[\varphi(kx,ky)-\varphi_w] + k_ok_1\right\} \tag{4}$$

$$A_o(kx,ky) = N(kx,ky)/D(kx,ky) \tag{5}$$

where B is a constant, ko is radar wavenumber, kx and ky correspond to wavenumber, aligned with and orthogonal to the IW propagation direction.

The initial implementation of this model considered predictions of spectral modulation for various choices of wind speed and direction, IW propagation speed, direction and current profile. These results were compared with results obtained by LB (Lyzenga, personal communication). Scenarios obtained in this investigation include aligned and opposing wind and IW propagation, as well as oblique angles of interaction. Our model considers both traditional 'relaxation' mechanisms (i.e. converging and diverging surface currents due to IWs), as well as modulation-related mechanisms and associated features (e.g. breaking and microscale breaking waves).

The spectral and modulation models discussed in this paper are available on the www for community-wide access (https://svn.apl.washington.edu/packages/sar_iw), though to access the site requires permission. This provides a useful platform for testing, verifying and comparing various Equilibrium Spectral models, as well as various models that express internal wave-surface wave (IW-SW) interactions. We have implemented three spectral models and two models for IW-SW modulation; both are described in some detail in the literature, so we provide only a brief overview in this paper.

2. Validation Database

To assist with model development and validation we assembled a database that includes collocated satellite data (ENVISAT, ERS, SAR imagery, SPOT imagery, and QuikScat wind vector maps), ship-based radar measurements (from the US-based R/V Revelle and the Taiwanese ship OR3), and moored thermistor chain (S7) measurements acquired in the South China Sea during the intensive data collection conducted in the summer of 2005 and off the coast of New Jersey in the summer of 2006. This database is complementary to the NLIWI project database (nliwi.org) and is one component of efforts to develop a forward model for predicting the sea surface patterns attributable to IWs and their corresponding SAR signatures.

IW events were found in all observational data including those acquired by ships, moored platforms and satellites including ENVISAT, ERS-2, and SPOT. Though IW events could be readily identified in individual data sets, there was a surprisingly limited number of cases where there were simultaneous ship-based and satellite-based or moored observations of IWs. A likely reason for the lack of collocations is that ship-based radars have a limited range (O(10 km)) relative to the scale of satellite imagery, so though considerable SAR imagery containing NLIWs were acquired during both experiments, the number of collocations is extremely limited due to constraints including time and location of satellite overpasses, direction of ship heading and radar look direction. Figure 3 provides an example of a collocated satellite- and ship-based observation of IWs; the ship-based radar data were acquired from the Taiwanese Research Vessel, the OR3.

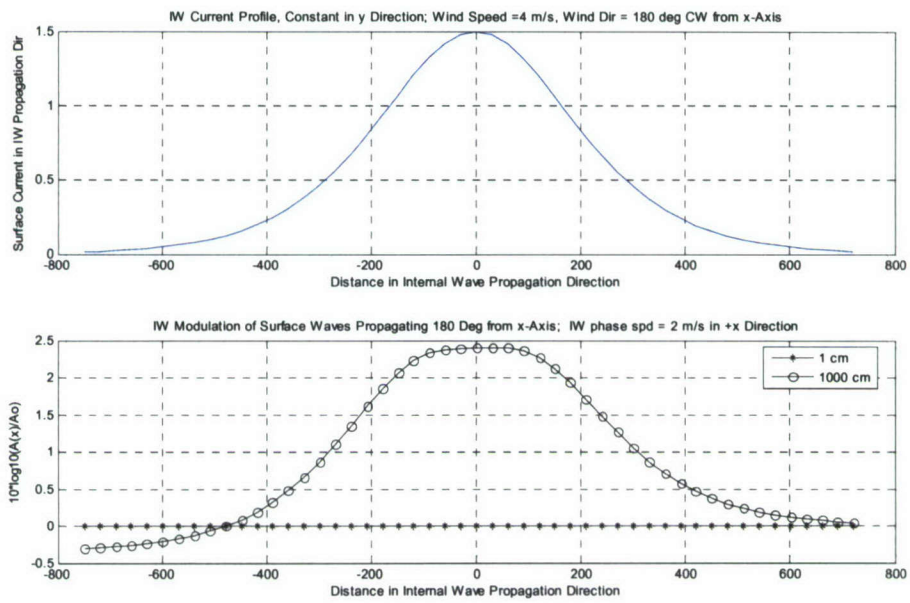

Figure 1. Modulation of equilibrium spectral density by currents due to NLIWs. Upper panel shows the surface currents in the direction of propagation of the NLIW; wind speed is 4ms^{-1}, and the NLIW propagation is directly opposing the wind. Lower panel shows the modulation (A/Ao) experienced by surface waves of 1 cm (*) and 10 m (o) due to interaction with the NLIW; 1cm (Bragg-scale) waves experience negligible modulation, whereas 10m waves experience significant modulation.

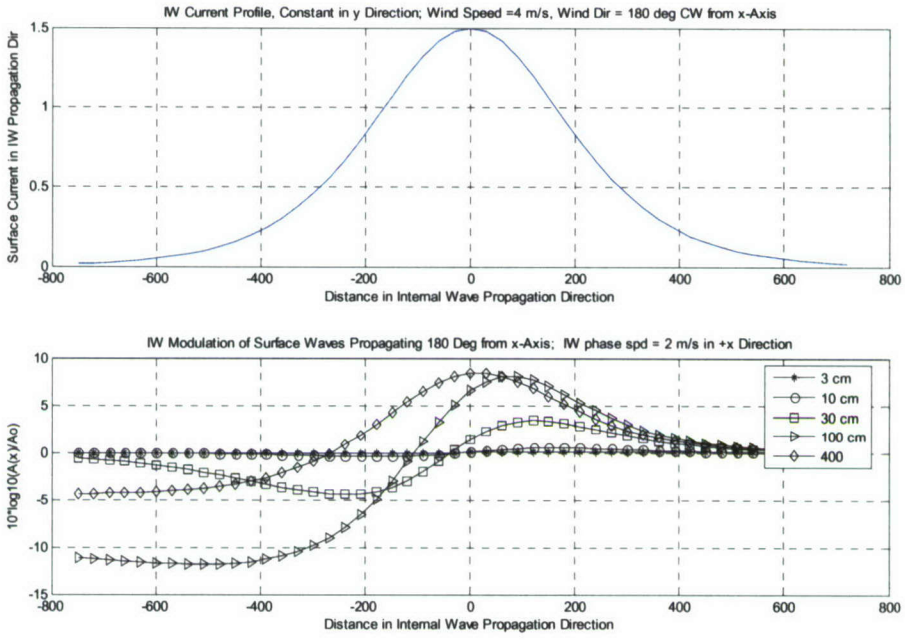

Figure 2. Modulation experienced by waves with wavelengths between the two extremes presented in Figure 1. Upper panel shows the surface current distribution for same conditions as in Figure 1. Lower panel shows the modulation (A/Ao) experienced by surface waves of 3 cm (*), 10 cm (o), 30 cm (square), 1m (triangle) and 4 m (diamond)due to interaction with the NLIW. Again the Bragg-scale waves (< 10 cm) experience negligible modulation, whereas the waves of 0.3, 1 and 4m experience significant and progressively increasing modulation.

3. Implementation

Our first step was to implement and then validate the LB model via qualitative and quantitative comparisons, which we accomplished successfully. Following preliminary implementation and validation, undesirable features were noted in the LB spectral model, particularly a singularity found at +/- $\pi/2$ relative to the wind direction. To avoid this feature we implemented an alternative version of this scheme that used the spectral model of Donelan and Pierson (1987) (hereafter referred to as DP) in the action modulation framework developed by LB. This model was selected for the following reasons: it was derived based on physical principles and measurements and has been used in many studies in radar remote sensing research. Also, at low wavenumbers, the DP model is identical to spectral model of Kudryavtsev et al.(1999), which is used in a subsequent part of this effort. The DP spectrum employs the same source terms and action modulation framework for computing SW-IW interactions as the LB model, but is more physically realistic.

The inputs to the LB model, for implementation of either the LB or DP spectral model includes: wind speed and direction, IW speed and direction, maximum surface current, current distribution, and current extent. Given these inputs, the LB model obtains the two-dimensional wavenumber spectra (in terms of energy, action or saturation, where

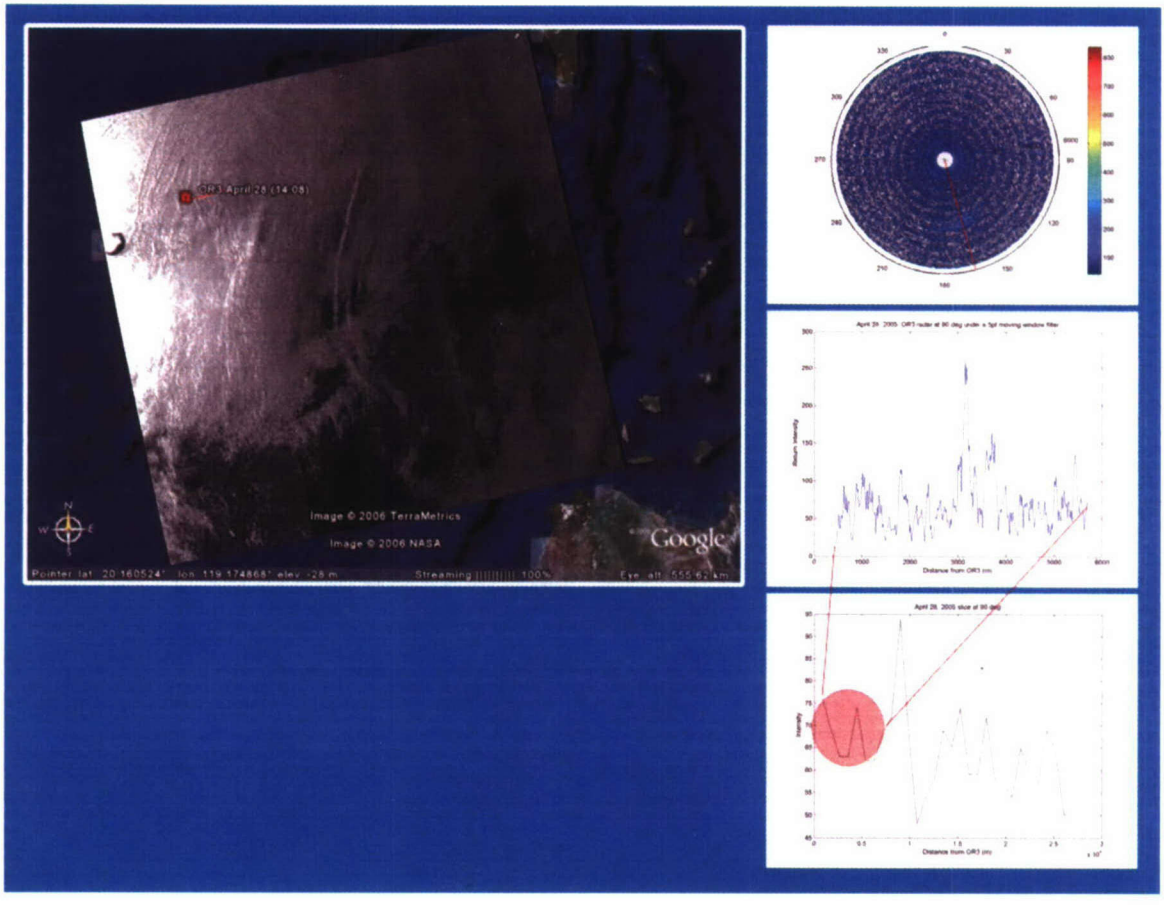

Figure 3. This figure shows collocated, satellite-based SAR and ship-based radar measurements of an internal wave in the South China Sea. This C-band, vertically polarized ENVISAT image was acquired April 28, 2005; wind speed was 0 – 2 ms^{-1} and from the SE, as estimated from a contemporaneous QuikScat overpass. The location of the OR3 is indicated in red in the upper left corner of the image. The three panels on the right of the figure show (top) an X-band ship-based radar measurement obtained from the OR3; (middle) an intensity plot taken in the direction of the IW (indicated by a red line in the top panel) that clearly shows the presence of an IW; (bottom) an intensity plot taken from the ENVISAT image along the direction indicated by the red line originating at the location of the OR3. The red shaded area shows the portion of the satellite-based intensity plot overlapping with the intensity plot for the ship-based radar. Though the resolution of the ENVISAT image is, as expected, much coarser than the ship-based radar, the same IW can still be clearly observed in both plots.

saturation, B, is given by $B(kx,ky) = k^4 S(kx,ky)$; k is wavenumber and S(kx,ky) is the wavenumber spectrum, and is a function of x- and y-wavenumber, as well as position along the internal wave, x, reflecting the modulation of the surface wave action with the passage of the IW.

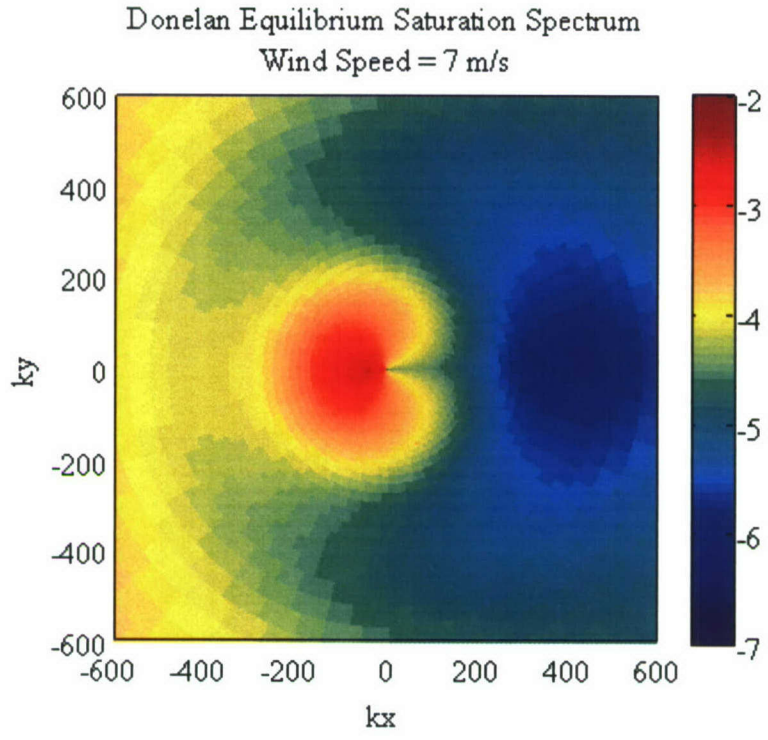

Figure 4 This shows the equilibrium spectral model of Donelan and Pierson (1987) for a wind of $7ms^{-1}$ blowing from right to left; the color bar shows spectral levels in dB.

An example of the Donelan and Pierson Equilibrium spectrum model is shown in Figure 4. Here, the wind speed is $7ms^{-1}$, wind direction is from the left to the right of the figure (from π), and the equilibrium spectrum is depicted in terms of saturation.

In addition to the LB scheme, we implemented an approach proposed by Kudryavtsev et al. (2003, 2005) for predicting IW-SW modulation. This approach uses the innovative spectral model of Kudryavtsev et al. (1999) and includes an action source term associated with the generation of parasitic capillary waves produced from the IW-SW interaction. An illustration of this spectral model is provided in Figure 5, for the same conditions (wind speed and direction) used to illustrate the DP model (Figure 4).

The action source terms used by Kudryavtsev (2003) are given in Equation 5.

$$Q(k) = \omega^3 k^{-5}\left[\beta_v(k)B(k) - B(k)\left(\frac{B(k)}{\alpha}\right)^n + I_{pc}(k)\right] \qquad (5)$$

The first term, $\beta_v(k) = \beta(k) - 4\nu k^2/\omega$ is 'effective growth rate', defined as wind growth rate less viscous dissipation, where β is given by

$$\beta(k) = C_\beta (u*/c)^2 \cos^2\varphi \qquad (6)$$

φ is the angle between wind and wave direction, and C_β is given by Stewart (1974). The second term of (5) expresses nonlinear wave-wave interaction; α and n are functions of k/k_g, where $k_\gamma = (g/\gamma)^{1/2} = k$ of minimum phase velocity, and $k_g = k_\gamma^2/k$;

The third term in expression (5) I_{pc} expresses the contribution of parasitic capillary waves to action modulation and is given by

$$I_{pc}(k) = \beta_v(k_g)B(k_g)\phi(k/k_g), \qquad (7)$$

where $\phi(k/k_g)$ is a filter function which restricts the action in k-space of source term $I_{pc}(k)$ to those gravity waves that generate parasitic capillaries. Figure 6 illustrates how I_{pc} works. The upper two panels show the wavenumber dependence of the terms α and n in the second action source term (in Equation 6). The bottom panel illustrates the wavenumber dependence of I_{pc}, which is essentially a filter function. I_{pc} will be nonzero when conditions are favorable for the generation of parasitic capillary waves by gravity waves.

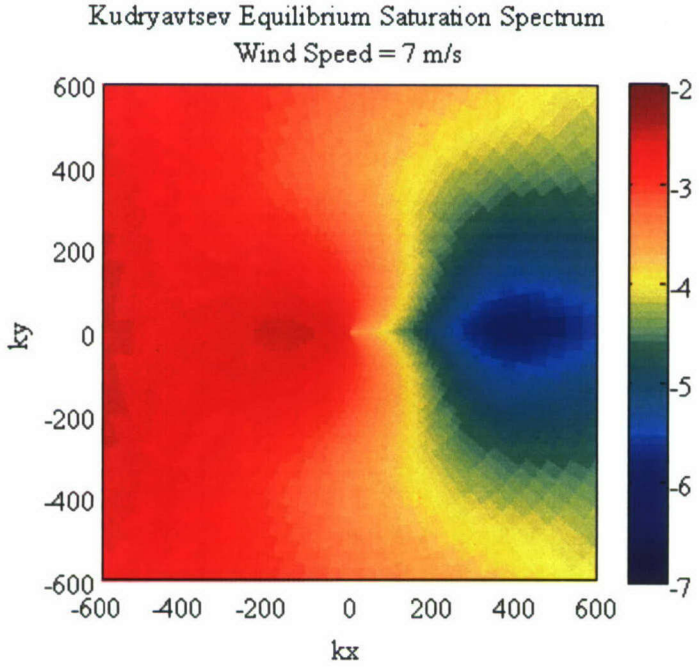

Figure 5 This shows the equilibrium spectral model of Kudryavtsev (1999) for a wind of $7ms^{-1}$ blowing from right to left; the color bar shows spectral levels in dB.

Variation of the I_{pc} source term with wavenumber is shown in Figure 7, which also illustrates the relative contribution of I_{pc} to the Kudryavtsev spectrum. The panel on the left shows the two dimensional wavenumber spectral model of Kudryavtsev et al. (1999) for a wind of 7ms-1, in the π direction (from right to left); the panel on the right illustrates the magnitude of the source term for parasitic capillary waves, I_{pc}, as a function

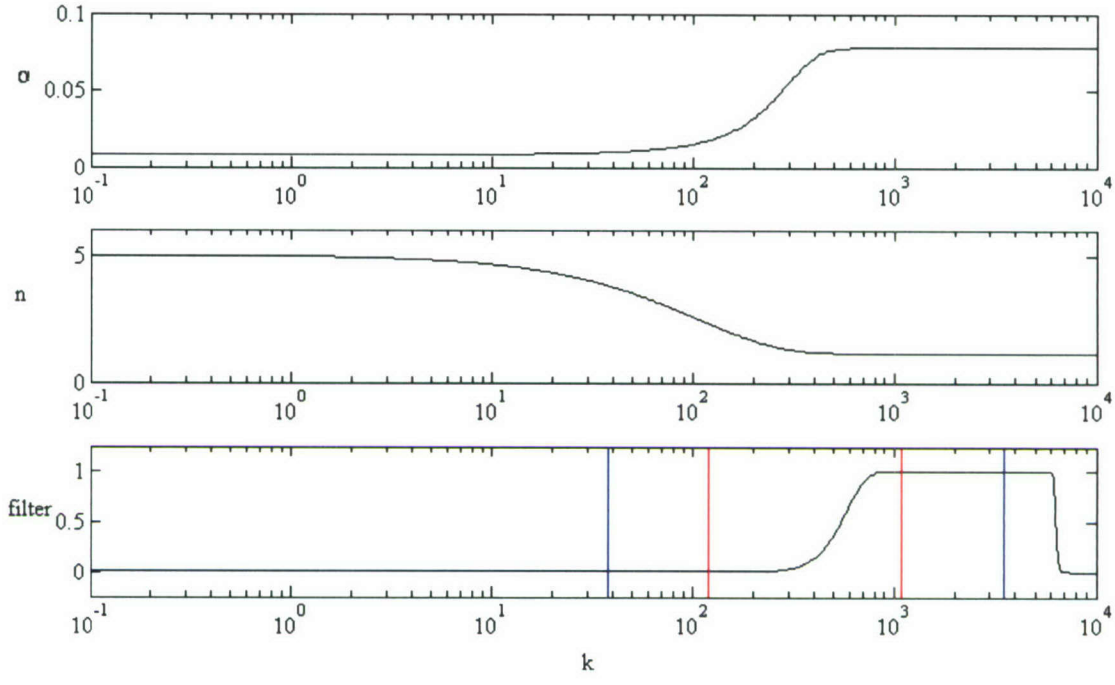

Figure 6 . Illustration of the wavenumber dependence of the exponent α (upper panel), and denominator n (middle panel), in the Kudryavtsev (2003) model's action source term for wave-wave interactions. The bottom panel shows the filter corresponding to the presence of parasitic capillary waves. The red and blue lines are included to show the relationship between gravity waves and corresponding parasitic capillary waves.

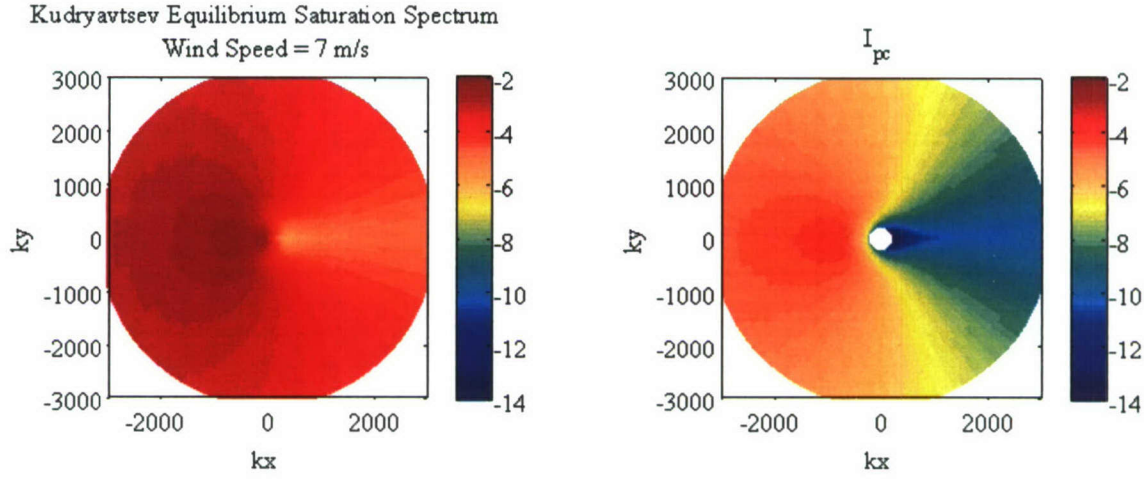

Figure 7 . Kudryavtsev (2003) equilibrium spectral model (saturation form) and corresponding action term associated with parasitic capillary waves, I_{pc}. Color bar shows relative power levels in dB.

of wavenumber and direction. Note that the range of wavenumbers illustrated in Figure 7 is expanded relative to what is depicted in Figure 5; the color bar (in dB) is also scaled to match the scaling of the source term associated with parasitic capillary waves, I_{pc}.

We compare the DP and Kudryavtsev (1999) equilibrium spectral models (i.e. not including SW-IW modulation effects) in Figure 8. Though not included in the analyses described here, it is worth noting that the 2-dimensional wavenumber spectrum serves as the inputs to electromagnetic scattering models used to predict the SAR signature of the sea surface. We intend to implement the stochastic, multiscale model of Plant (2004), and will compare model-based predictions with satellite- and ship-based radar measurements as part of model validation. Recall that the two approaches (LB action computation with DP spectral model, and Kudryavtsev modulation and spectral model) use different action source terms and different computational schemes.

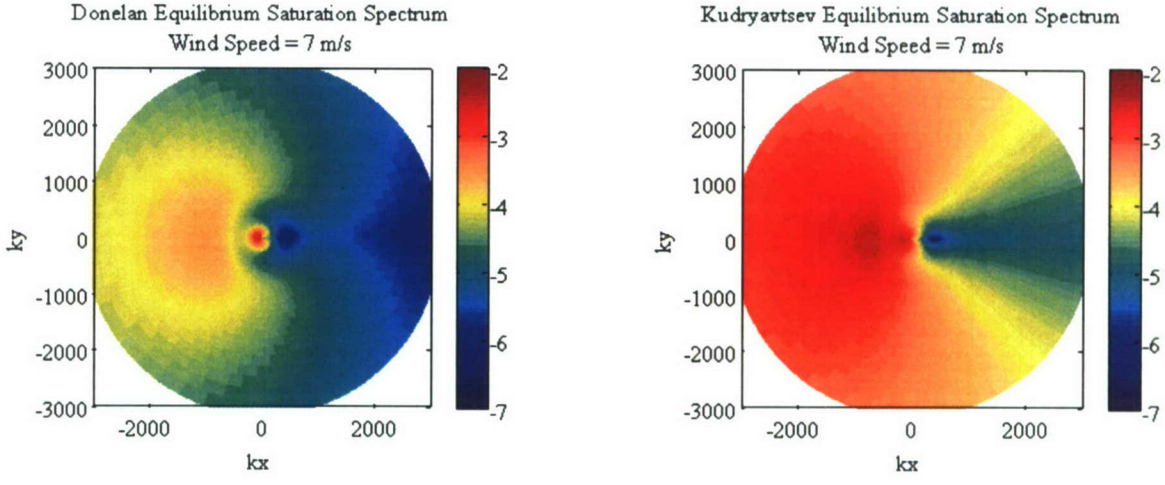

Figure 8 2-Dimensional wavenumber spectral model of Donelan et al. (1985), left panel, and Kudryavtsev et al. (1999), right panel, for wind speed 7ms^{-1}; wind direction = π. Color bar shows relative power in dB. *Note color bar is different in Figures 7 and 8.*

Figures 9 and 10 enable us to compare the modulated spectrum at various locations along a current profile produced by a hypothetical IW for both the DP/LB model and the Kudryavtsev model. In these examples, we assume the current profile has a sech^2 shape, extends over 3 km (from -1500 m to + 1500 m), and attains a maximum of 0.7 ms^{-1}, as illustrated in the bottom-most panel of each figure. The indices A – D assigned to the upper panels of the figure correspond to location along the current profile shown in the lower panel. The spectrum at location D will be similar, but not identical to the equilibrium (unmodulated) spectrum, Ao.

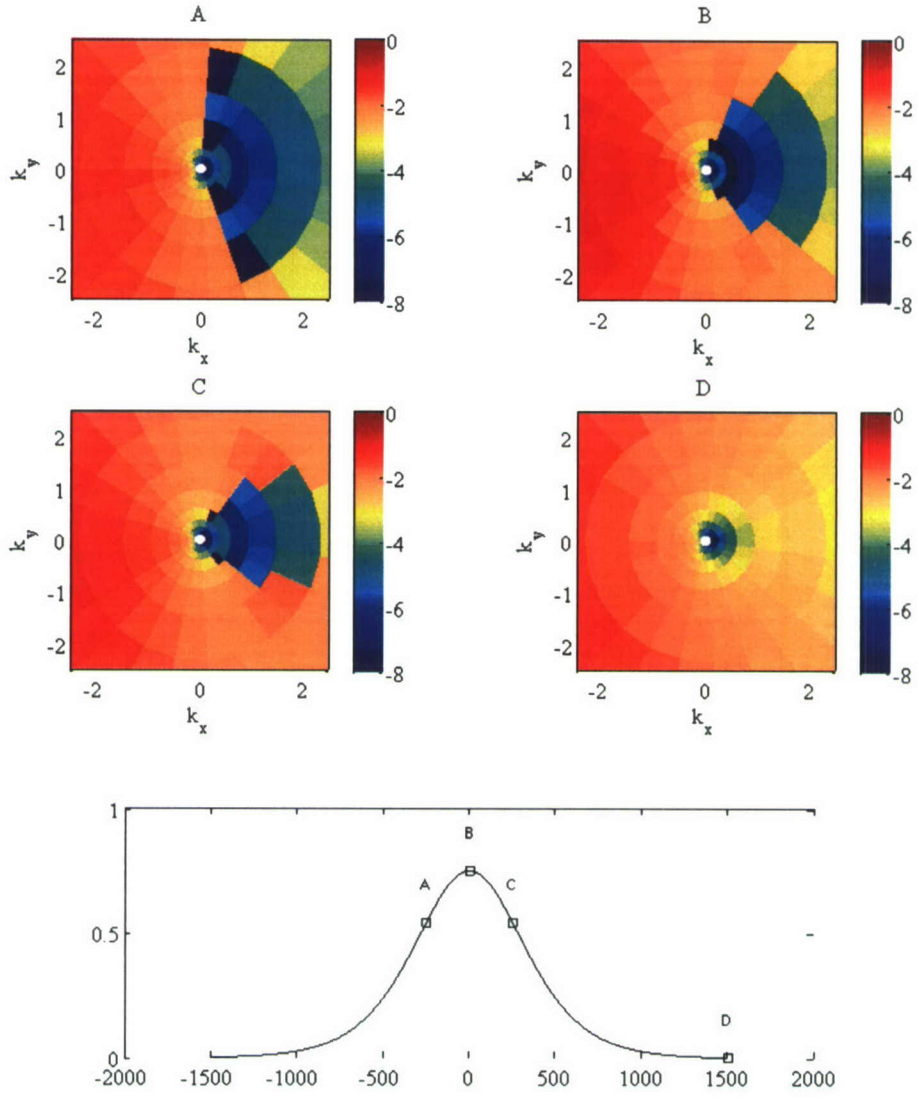

Figure 9. Upper four panels illustrate the impact of IW-SW modulation on surface waves distributed according to the Donelan and Pierson (1987) spectral model. Model results are provided corresponding to surface waves between 62 m 2.5 m wavelength. We focus here on intermediate-scale waves, as the LB model assumes (as shown in Figures 1 and 2) that IWs directly modulate centimeter-scale (Bragg) waves. The color bar shows the saturation spectrum (in dB) corresponding to the four locations indexed by letters A-D.

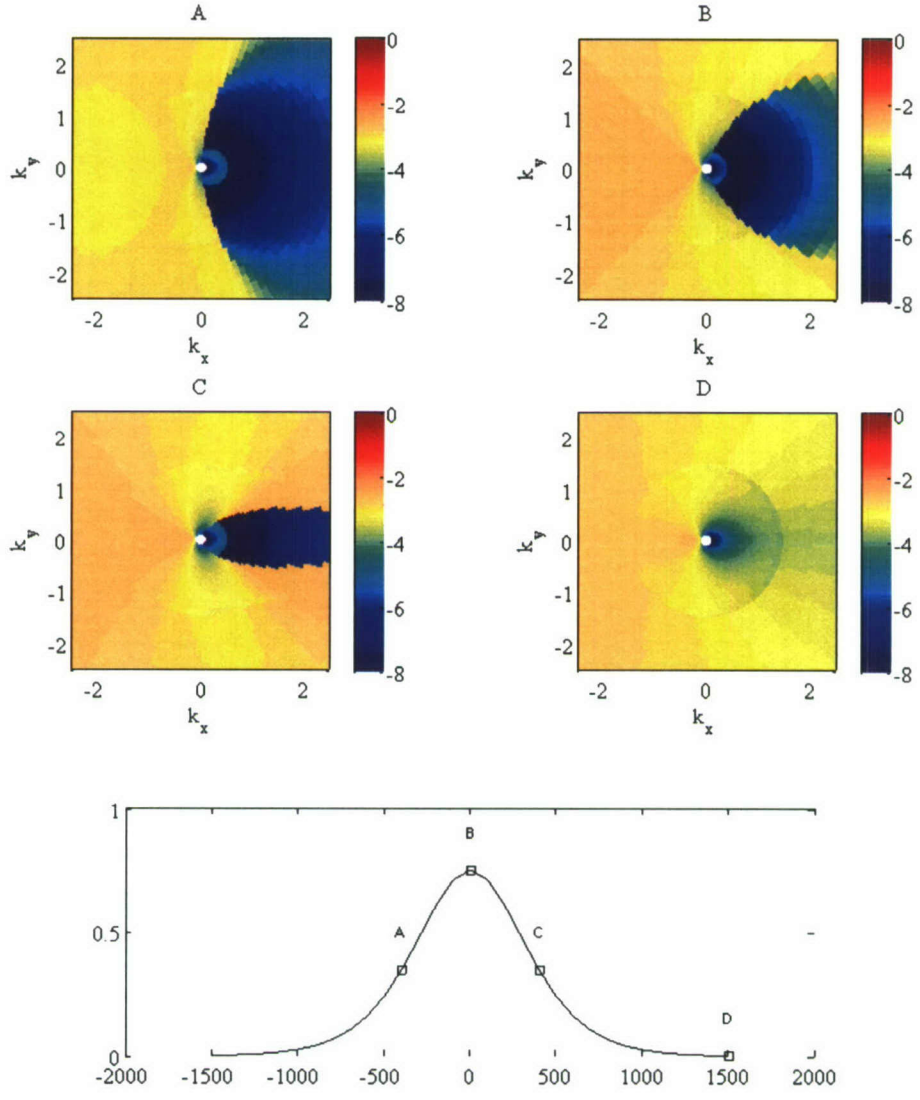

Figure 10. As in Figure 9, the upper four panels illustrate the impact of IW-SW modulation on surface waves distributed according to the Kudryavtsev (1999) spectral model. Model results are provided corresponding to surface waves between 62 m 2.5 m wavelength. We focus here on intermediate-scale waves, as the Kudryavtsev model also assumes that IWs directly modulate centimeter-scale (Bragg) waves. The color bar shows the saturation spectrum (in dB) corresponding to the four locations indexed by letters A-D.

During the field experiment held off the coast of New Jersey in the summer of 2006, surface current velocity estimates were obtained from the R/V Oceanus (J. Moum, personal communication) that revealed the current structure shown in Figure 11. An analytical fit (D. Lyzenga, personal communication) was obtained for these data, which corresponds to the red line superimposed on the blue data plot. It is believed that the $sech^2$-type current profile shown in Figures 9 and 10 corresponds to IW characteristics typically observed in the South China Sea; current profiles such as shown in Figure 11 correspond to what is frequently observed off the coast of New Jersey. In Figures 12 and 13 we look at the IW-SW modulation in different wavenumber regimes produced by a current profile similar to that shown in Figure 11.

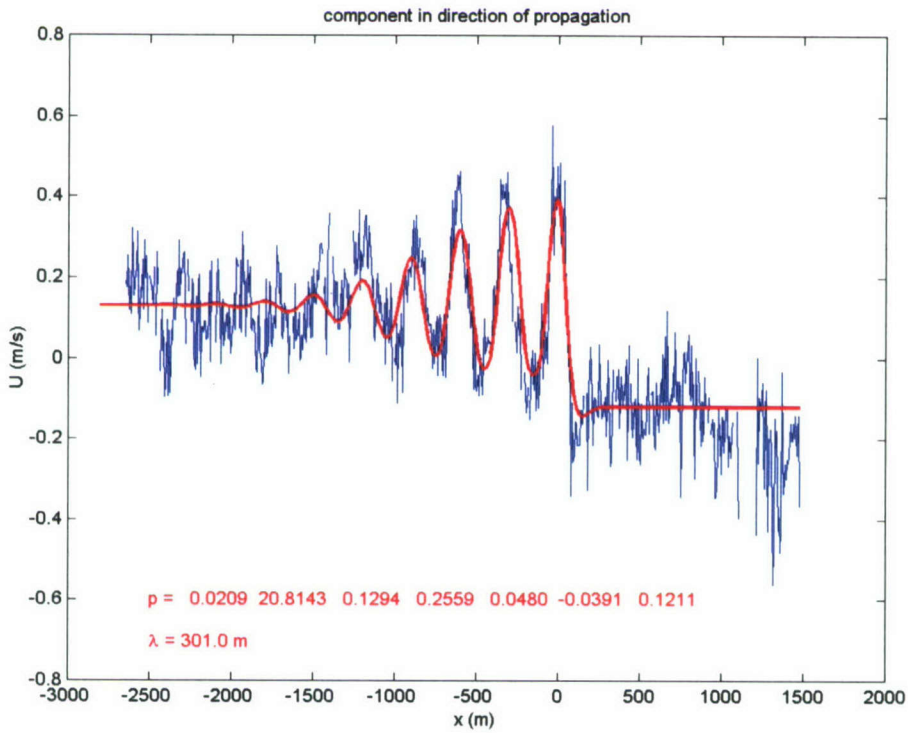

Figure 11 Surface current estimates for a train of internal waves observed off the coast of New Jersey in summer 2006, extrapolated to the surface from ADCP measurements on the R/V Oceanus (courtesy of J. Moum for observational data, and D. Lyzenga for the extrapolation). Blue lines indicate observed data; heavy red lines correspond to a polynomial fit to the data; coefficients noted on the lower edge of the plot. These current estimates are used in Figures 12 and 13 to modulate the surface wave spectra.

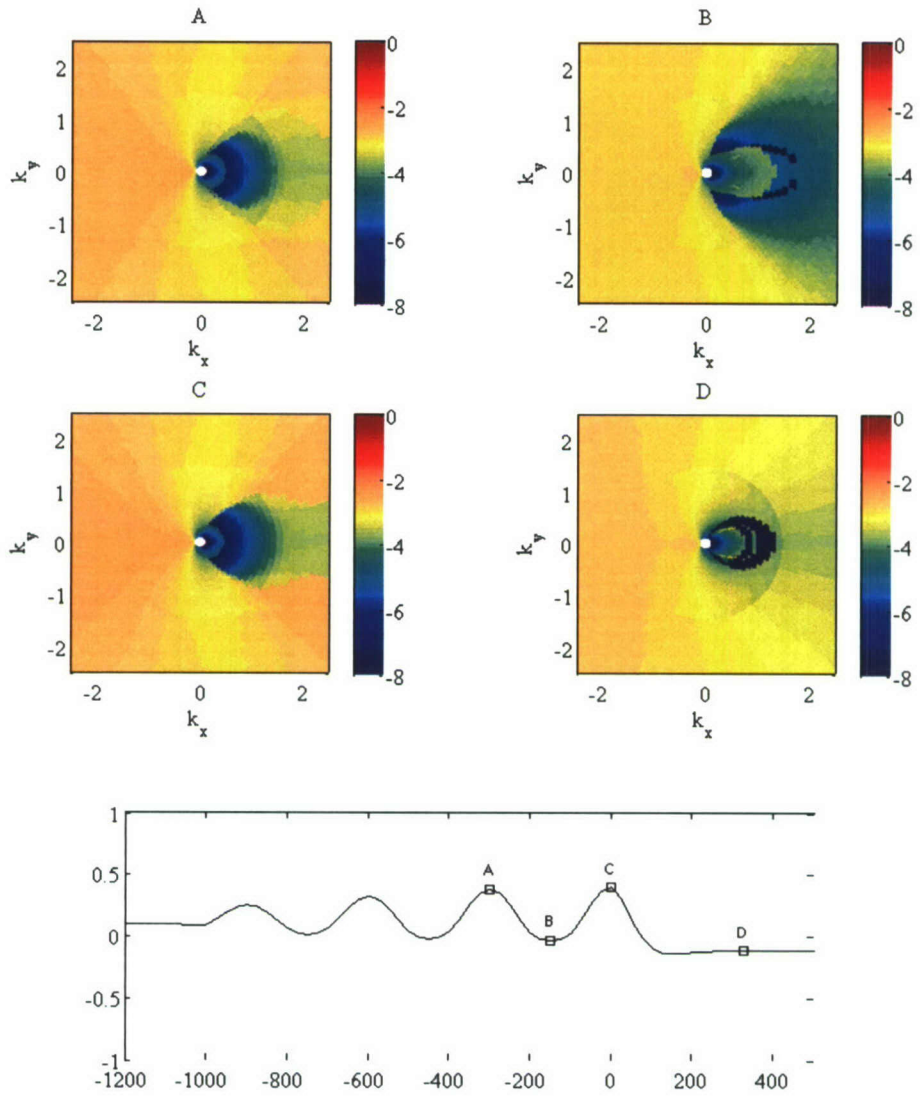

Figure 12 Here we can examine IW-SW modulation of the Kudryavtsev spectrum for wavenumbers between 0.1 and 2.5 (wavelengths between 62.5 m and 2.5 m). Panels A – D show modulated SW spectrum at various locations along an IW current profile (shown in bottom panel); letters designate locations where spectra are obtained. Color bar shows spectral saturation levels in dB.

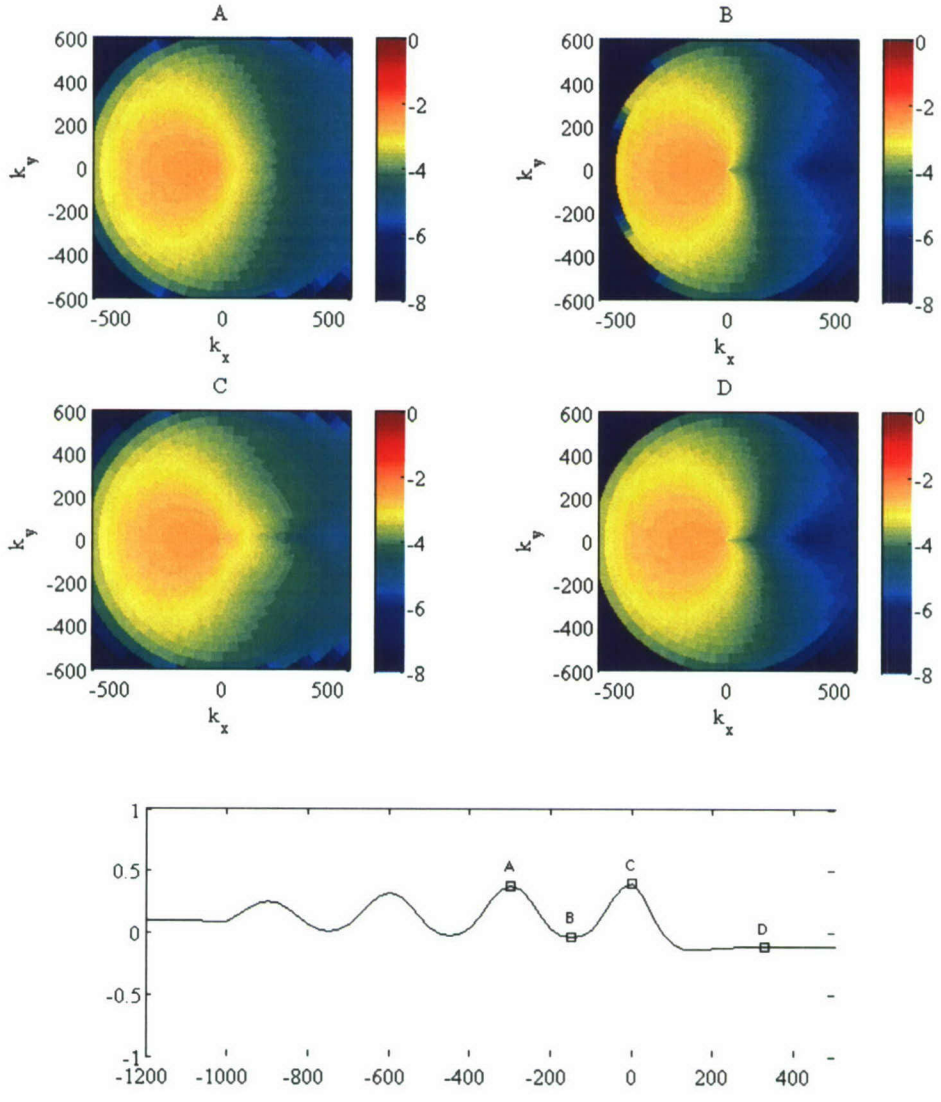

Figure 13 Here we consider IW-SW modulation of the Kudryavtsev spectrum for a much broader range of wavenumbers between 0.1 and 500 (wavelengths between 62.5 m and 0.01 m). Panels A – D show modulated SW spectrum at the same locations along an IW current profile as were considered for Figure 12; letters designate locations where spectra were obtained; again locations are indicated in bottom panel. Color bar shows spectral saturation levels in dB.

SUMMARY

We have successfully applied the spectral models of Lyzenga and Bennett (1988), Donelan and Pierson (1987) and Kudryavtsev et al. (1999, 2003), as well as the action modulation frameworks of Lyzenga and Bennett and Kudryavtsev (2003). We used the various techniques to study the modulation of surface waves by internal waves. As Figures 9 – 13 demonstrate, we were able to show that there is considerable IW-SW modulation, but none of the approaches implemented thus far are completely satisfactory. For example, the model of Kudryavtsev et al. assumes that the longer waves produce parasitic capillary waves, but small-scale breakers are considered to be sources of short waves in the action conservation equations. But these equations are usually solved assuming that the short waves move at their intrinsic phase speeds, an assumption that is not correct for short waves that are being advected by longer ones, let alone for those that are forced by the longer waves. Furthermore, models for predicting backscatter require us to know where on longer waves the breakers and parasitic capillaries are located, and this cannot be determined with the present approach.

NEXT STEPS

While the work described in this paper has made considerable progress towards understanding IW-SW modulation, and towards predicting the surface manifestations of this phenomenon, there is clearly considerable work still to be done. Additional physical effects need to be incorporated into the spectral models and action modulation framework models. Plant has proposed to follow on the research described in this report with a new approach where parasitic capillaries and breaking wave patches are considered distortions of longer waves in the scattering model, rather than being included in the action conservation equations. Also, a more recent paper by Kudryavtsev et al. (2005) considers action modulation to arise from wind forcing, viscous effects, dissipation via wave breaking, wave-wave interactions, generation of free waves by breaking waves, and generation of bound (parasitic) capillary waves by breaking waves. While this approach looks promising, it does not address the concerns raised above regarding short wave advection by longer waves.

Additional next steps we hope to validate the models described in this report are to compare predictions of IW-SW modulation with measurements from ASIS buoys (Hans Graber, personal communication) deployed during field experiments in regions where significant IW activity is anticipated, e.g. South China Sea or off the coast of New Jersey. In addition to comparisons of direct measurements, we would like to compare predictions of σ^0 (radar backscatter) based on with ship- tower- or satellite-based radar measurements for a variety of current configurations. Final improvements we hope to implement include prediction of modulation from currents that vary both in x and y; interactions involving SW, IW and swell, and implementation of a faster, more efficient version of the code.

BIBLIOGRAPHY

Donelan M.A. and W.J, Pierson, 1987, Radar scattering and equilibrium ranges in wind-generated waves with application to scatterometry, J. Geophys. Res., 92(C5),4971-5029

Kudryavtsev V., V.Makin, and B. Chapron, 1999, Coupled sea surface atmosphere model, 2, Spectrum of short wind waves, J. Geophys. Res., 104, 7625-7639

Kudryavtsev V., D. Hauser, G. Caudal, and B. Chapron, 2003, A semi-empirical model of the normalized radar cross-section of the sea surface: 1. The background model, J. Geophys. Res., 108(c3), 8054, doi:10.1029/2001JC001003

Kudryavtsev V., D. Akimov, J. Johannessen and B. Chapron, 2005, On radar imaging of current features: 1. Model and comparison with observations, J. Geophys. Res., 110 (c07016), doi:10.1029/3004JC002505

Lyzenga D.R. and J. M. Bennett, 1988, Full-spectrum modeling of synthetic aperture radar internal wave signature, J. Geophys. Res., 93(c10), 12,345-12,354

Phillips O.M., 1980, The Dynamics of the Upper Ocean, 2nd ed., Cambridge University Press, 336 pp.

Plant WJ, 2002, A stochastic, multiscale model of microwave backscatter from the ocean, J. Geophys. Res.,107(C9), 3120, doi:10.1029/2001JC000909.

Plant W.J., 1982, A relationship between wind stress and wave slope, J. Geophys. Res., 87, 1961-1967.

Stewart, R.W., 1974, The air-sea momentum exchange, Boundary Layer Meteorol., 6, 151-167

REPORT DOCUMENTATION PAGE

Form Approved
OMB No. 0704-0188

PLEASE DO NOT RETURN YOUR FORM TO THE ABOVE ADDRESS.

1. REPORT DATE *(DD-MM-YYYY)*	2. REPORT TYPE	3. DATES COVERED *(From - To)*
04/08/2008	Final Report	21 Feb 2005 to 30 Sept 2007

4. TITLE AND SUBTITLE

Modeling the SAR Signature of Nonlinear Internal Waves

5a. CONTRACT NUMBER

5b. GRANT NUMBER

N00014-05-1-0368

5c. PROGRAM ELEMENT NUMBER

6. AUTHOR(S)

Ellen E. Lettvin

5d. PROJECT NUMBER

5e. TASK NUMBER

5f. WORK UNIT NUMBER

7. PERFORMING ORGANIZATION NAME(S) AND ADDRESS(ES)

Applied Physics Laboratory - University of Washington
1013 NE 40th Street
Seattle, WA 98105-6698

8. PERFORMING ORGANIZATION REPORT NUMBER

9. SPONSORING/MONITORING AGENCY NAME(S) AND ADDRESS(ES)

Office of Naval Research (ONR 322)
875 North Randolph Street
Arlington, VA 22203-1995

10. SPONSOR/MONITOR'S ACRONYM(S)

ONR

11. SPONSOR/MONITOR'S REPORT NUMBER(S)

12. DISTRIBUTION/AVAILABILITY STATEMENT

Distribution A, Unrestricted

13. SUPPLEMENTARY NOTES

None

14. ABSTRACT

Nonlinear Internal Waves are pervasive globally, particularly in coastal waters. The currents and displacements associated with internal waves influence acoustic propagation and underwater navigation, as well as ocean transport and mixing. Synthetic Aperture Radar (SAR) imagery can reveal the surface manifestations of internal waves (IWs) in satellite imagery and so is routinely used to locate and characterize these features. Though some of the mechanisms that link the SAR signatures, surface processes, and the underlying internal structures have been understood for decades, a complete characterization has yet to emerge, making SAR imagery useful only as a qualitative tool. The objective of this research is to develop and validate a forward model to predict the SAR signature of NLIWs that explicitly includes relevant mechanisms that impact the sea surface roughness and corresponding backscattering cross section, such as wind speed and direction, compound modulation (i.e. modulation of intermediate-scale waves by IWs, which in turn modulate smaller waves), microscale breaking and breaking waves.

15. SUBJECT TERMS

synthetic aperture radar, nonlinear internal waves, forward models, modulation, sea surface temperature, internal wave-surface wave interaction

16. SECURITY CLASSIFICATION OF:			17. LIMITATION OF ABSTRACT	18. NUMBER OF PAGES	19a. NAME OF RESPONSIBLE PERSON
a. REPORT	b. ABSTRACT	c. THIS PAGE			Dr. Theresa Paluzxkiewicz (ONR)
U	U	U	UU	16	19b. TELEPHONE NUMBER *(Include area code)* 703-696-6680